

Audio-Driven Reinforcement Learning for Head-Orientation in Naturalistic Environments

Wessel Ledder 

Radboud University

Nijmegen, Netherlands

Yuzhen Qin 

Donders Institute, Radboud University

Nijmegen, Netherlands

Kiki van der Heijden 

Donders Institute, Radboud University

Nijmegen, Netherlands

Mortimer B. Zuckerman Mind Brain Behavior Institute

Columbia University, New York, United States

Abstract—Although deep reinforcement learning (DRL) approaches in audio signal processing have seen substantial progress in recent years, audio-driven DRL for tasks such as navigation, gaze control and head-orientation control in the context of human-robot interaction have received little attention. Here, we propose an audio-driven DRL framework in which we utilise deep Q-learning to develop an autonomous agent that orients towards a talker in the acoustic environment based on stereo speech recordings. Our results show that the agent learned to perform the task at a near perfect level when trained on speech segments in anechoic environments (that is, without reverberation). The presence of reverberation in naturalistic acoustic environments affected the agent’s performance, although the agent still substantially outperformed a baseline, randomly acting agent. Finally, we quantified the degree of generalization of the proposed DRL approach across naturalistic acoustic environments. Our experiments revealed that policies learned by agents trained on medium or high reverb environments generalised to low reverb environments, but policies learned by agents trained on anechoic or low reverb environments did not generalise to medium or high reverb environments. Taken together, this study demonstrates the potential of audio-driven DRL for tasks such as head-orientation control and highlights the need for training strategies that enable robust generalization across environments for real-world audio-driven DRL applications.

Index Terms—Deep reinforcement learning, head-orientation control, human-robot interaction, spatial audio processing.

I. INTRODUCTION

For natural human-robot interaction, eye-contact between a robot and a talker is an important nonverbal signal [1], [2]. Eye contact is established through gaze direction and head orientation, both of which can be controlled in robotics using deep reinforcement learning techniques (DRL, [3]). Yet, very few DRL approaches have been proposed for gaze control [4] and, to the best of our knowledge, none for head-orientation control.

In contrast, DRL for robot navigation - a related, comparable task - has received widespread attention [5]. Most DRL approaches in the field of robot navigation operate on visual input (e.g. [6], [7]), or on multi-modal audio-visual input (e.g. [8], [9]). While these multi-modal DRL approaches demonstrated that providing audio signals improves an agent’s

This project received funding from the NWO Talent Program under the Veni grant agreement VI.Veni.202.184 (KH). This publication is also part of the Dutch Brain Interface Initiative (DBI2) with project number 024.005.022 of the NWO Gravitation research programme (YQ).

navigation performance in comparison to providing visual signals only, pure audio-driven approaches for robot navigation are much less prevalent [10], [11]. Further, despite the increase in RL applications in the field of audio signal processing [12], exclusively audio-driven RL approaches have not been investigated for gaze or head-orientation control. The potential of DRL techniques for creating audio-driven autonomous systems that learn directly from sound signals in the environment [12] thus remains largely unexplored for applications such as navigation, gaze control, and head-orientation.

Here, we propose an audio-driven DRL approach for head-orientation control in the context of human-robot interaction. We use deep Q-learning [13] with a recurrent neural network (RNN) architecture to develop an agent that learns a policy for orienting its head towards a talker in the acoustic environment. The agent is trained on spatialized stereo speech recordings which contain human spatial cues [14]. We simulate several acoustic environments (anechoic, low reverb, medium reverb and high reverb) to assess the impact of reverberation on task performance and to assess generalization across a range of naturalistic acoustic environments. Specifically, as reverberation is known to have a strong impact on human hearing (including sound localisation, [14]) as well as on machine hearing (for example, speech separation [15]), obtaining a measure of generalization across diverse naturalistic environments is crucial for future development of real-world applications [16].

Our results show that our proposed DRL agent can robustly learn head-orientation control from stereo speech recordings in a range of acoustic environments. These findings highlight the potential of audio-driven DRL approaches for the current task, as well as a wide range of other tasks, such as robot navigation.

II. NATURALISTIC ACOUSTIC SCENES

A. Dataset

We applied our audio-driven DRL approach to anechoic speech scenes and to naturalistic, reverberant speech scenes. Speech clips (10 s duration) were selected from the LibriSpeech database [17]. We selected 30 speech clips for each of 40 randomly sampled talkers to generate the training set and 20 clips of 10 different talkers to generate an independent test set. We presented the selected speech clips at 64 talker locations in the frontal hemifield: 13 azimuth locations ranging

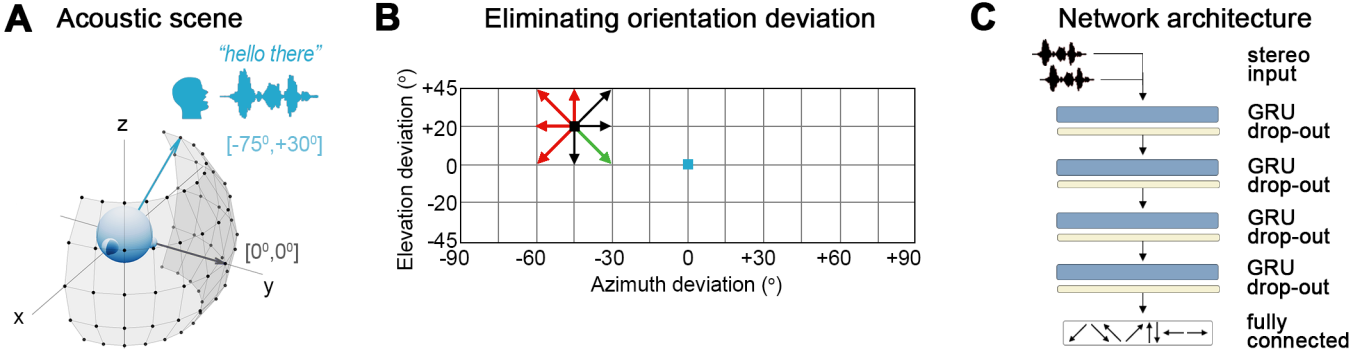


Fig. 1. (A) Schematic illustration of an acoustic scene and the head orientation task. Black arrow: agent's head orientation at the start of the episode. Blue arrow: target head orientation. The grid reflects all possible talker locations. (B) We define the head orientation problem as a task in which the aim is to eliminate the orientation deviation between the direction of arrival of the talker's voice and the agent's head orientation. As such, we can define a 2D grid in which orientation deviation is expressed in terms of the azimuth and elevation deviation. The blue square indicates the target orientation deviation in all episodes ($0^\circ, 0^\circ$). The black square represents an example of an agent's orientation deviation with respect to the talker's location. Arrows indicate possible actions. Green arrow: optimal action (largest decrease in orientation deviation). Red arrows: non-optimal actions (increase in orientation deviation). Black arrows: all other actions. (C) Schematic overview of the recurrent neural network architecture used to approximate the optimal action-value function.

from -90° to $+90^\circ$ in equidistant steps of 15° and 5 elevation locations ($-45^\circ, -20^\circ, 0^\circ, +20^\circ$ and $+45^\circ$). Talker location $[0^\circ, 0^\circ]$ was excluded as this location corresponds to the agent oriented towards the talker.

B. Anechoic acoustic scenes

To spatialize sound clips to a given location in an anechoic environment (that is, without reverberation), we convolved each monaural speech clip with a head related transfer function (HRTF) from the SOFA HRTF library [18]. HRTFs capture listener-specific acoustic properties and simulate human binaural listening to a source at a specific location in an anechoic environment (at 1.5 m distance).

C. Naturalistic acoustic scenes with reverberation

We simulated naturalistic, reverberant rooms using binaural room impulse responses (BRIRs). First, we calculated Room Impulse Responses using PyroomAcoustics [19] for three rooms that varied in size: small ($4\text{ m} \times 6\text{ m} \times 4\text{ m}$), medium ($5\text{ m} \times 7\text{ m} \times 4\text{ m}$) and large ($6\text{ m} \times 8\text{ m} \times 4\text{ m}$). Each room was coupled with a T_{60} based on the size of the room to simulate an increasing amount of reverberation with increasing room size: T_{60} small room = 0.2, T_{60} medium room = 0.4 and T_{60} large room = 0.6. The listener was positioned centrally in the room. For each room, we generated 64 RIRs corresponding to the 64 talker locations, as well as a RIR for target location $[0^\circ, 0^\circ]$. This resulted in a total of 65 RIRs per room.

Next, we computed BRIRs by convolving the RIRs with the HRTFs using Binaural SDM [20]. For all RIR, we calculated a BRIR for each of the 65 talker locations and all possible head orientations of the agent. The agent's head orientation was restricted to the same range as the talker locations, that is, to 65 head orientations. In total, we generated 4,225 BRIRs per room. Finally, we convolved the BRIRs with the monaural speech clips to create stereo clips of spatialized talkers in naturalistic, reverberant environments.

III. AUDIO-DRIVEN REINFORCEMENT LEARNING APPROACH

A. Problem statement

Our goal is to find the shortest sequence of actions that orients the head of an agent from its starting position towards the direction of arrival of a talker's voice, such that the agent directly faces the talker (Fig. 1 A). We define this problem in terms of the orientation deviation between the agent's head and the talker's location in the environment in which the agent's objective is to eliminate the orientation deviation (OD). Fig. 1 B shows a 2-dimensional grid visualization of the task.

OD is defined as the Euclidean distance between the direction of arrival of a talker's voice (V), $[azimuth_V, elevation_V]$, and the head orientation of the agent (HOA), $[azimuth_{HOA}, elevation_{HOA}]$:

$$OD = \sqrt{(\Delta azimuth)^2 + (\Delta elevation)^2} \quad (1)$$

To achieve this goal, we developed a deep reinforcement learning approach which takes as input a stereo speech clip and outputs an action in 2D space. The action space consists of eight possible actions: rotating left, right, up, down, or diagonal (Fig. 1 B).

B. Reinforcement learning

We formulated the head-orientation task as a partially observable Markov Decision Process (POMDP) [21], [22] in which the agent interacts with the acoustic environment through observations, actions and rewards. The POMDP is defined as the tuple $(\mathcal{S}, \mathcal{A}, \mathcal{R}, \mathcal{P}, \mathcal{O}, \Omega, \gamma)$ in which at each time step $t \in [0, T]$, the agent receives as input observation $o_t(s_t) \in \mathcal{O}$, which informs the agent about the state of the environment $s_t \in \mathcal{S}$. In our case, the observations are the segments of a speech clip. Based on the observation, the agent selects action $a_t \in \mathcal{A}$ following policy π , that is, $a_t = \pi(o_t)$ and receives reward $r(s_t) \in \mathbb{R}$. The agent then transitions

TABLE I
PERFORMANCE OF THE RL AGENT IN ITS TRAINING ENVIRONMENT.

Environment	Success rate (%)	Chebyshev distance	Episode length
Random	27.6	2.8	17.3
Anechoic	100	0.0	4.3
Low reverb	66.7	0.5	12.7
Med reverb	57.3	0.9	13.9
High reverb	57.8	0.8	13.7

into the next state $s_{t+1} \in \mathcal{S}$ with probability $p(s_{t+1}|s_t, a_t)$ and observe $o_{t+1} \in O$ with probability $\Omega(o_{t+1}|s_{t+1})$. Note that the states to which the agent can transition, depend on its current state: $\mathcal{S}_t \subset \mathcal{S}$ denotes the set of possible states the agent can reach from the current state s_{t-1} . The aim of the reinforcement learning paradigm is to learn policy π which maximizes the cumulative reward discounted by discount factor γ .

We utilised a semi-dense reward scheme in which the agent received a reward r_t after each action a_t in order to encourage the agent to learn the shortest sequence of actions to orient towards the target. To allocate this immediate reward, we compared the new orientation deviation $OD(s_{t+1})$ with the one at the previous step. Specifically, we let

$$r(s_t, a_t, s_{t+1}) = \begin{cases} +0.1, & \text{if } OD(s_{t+1}) = \min_{s \in \mathcal{S}_{t+1}} OD(s), \\ -0.2, & \text{if } OD(s_{t+1}) > OD(s_t), \\ 0 & \text{otherwise.} \end{cases} \quad (2)$$

Finally, a reward r_{target} of +1 was assigned upon reaching the target. If the target was not reached, the episode terminated when the agent reaches the maximum number of 20 actions.

C. Deep Q-Learning

We utilise a deep Q-network approach [13] to train the agent. At each time step t , the training loop updates predicted Q-values towards target Q-values. At the start of the training loop, the agent interacts with the environment by making observation o_t and taking action a_t based on an ϵ -greedy policy and current Q-values. The agent's experiences $e_t = (o_t, a_t, r_t, o_{t+1})$ are stored in memory replay buffer $D_t = e_0, \dots, e_t$. To ensure that equal importance is given to transitions at all orientation deviations, we structured the memory buffer by talker location with a size of 5,000 experiences per orientation deviation. This resulted in a total memory buffer size of 325,000 experiences.

The weights of the policy network $Q(o, a; \theta)$ are updated in an optimization step. To this end, we sample experiences uniformly and at random across orientation deviations from the memory replay buffer $(o, a, r, o') \sim U(D)$. Q-values are updated at iteration i based on the Huber loss [23], which seeks to minimize:

$$L_i(\theta_i) = \mathbb{E}_{o, a, r, o' \sim U(D)} \left[\text{Huber} \left(r + \gamma \max_{a'} Q(o', a'; \theta_t^-) - Q(o, a; \theta_i) \right)^2 \right] \quad (3)$$

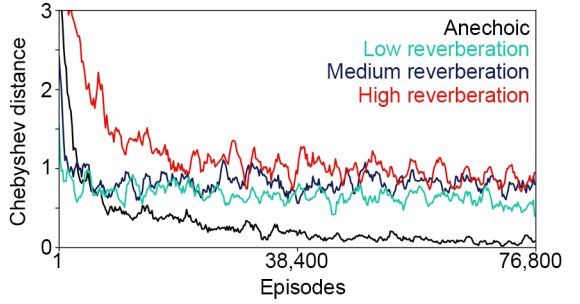


Fig. 2. Temporal evolution of Chebyshev distance during training in anechoic and reverberant environments.

We periodically adjust the target Q-values to reduce correlations between the actual Q-values and the target Q-values. To this end, we perform a soft update of the parameters of target network θ^- by the policy network parameters θ every C steps [24].

D. Network architecture

We utilised a recurrent neural network (RNN) model to approximate the optimal action-value function. The network consisted of four GRU layers (512, 256, 128 and 64 nodes, respectively). GRU layers were followed by a drop-out layer (drop-out rate = 20 % for layer 1 - 3 and 50 % for layer 4). The final drop-out layer was followed by a fully-connected linear layer with eight outputs corresponding to the action space (Fig. 1 C).

E. Episodes

At the start of an episode, the selected 10 s speech clip was divided in 20 windows of 500 ms. The first window of 500 ms served as s_0 and was spatialized to a randomly sampled talker location in the acoustic environment. The head orientation of the agent was always $[0^\circ, 0^\circ]$ at the start of an episode. After the agent performed action a_t , thereby rotating its head into a particular direction, the next state s_{t+1} was generated by taking the next window of 500 ms of the speech clip and spatializing this according to the new head orientation of the agent. An episode was terminated when $OD = 0.0$ or when the maximum number of actions was reached.

F. Hyperparameters

We prepared and trained the network with the Pytorch framework [25], using the AdamW Optimizer [26], a learning rate of 0.001 and a batch size of 1024. We set discount factor γ to 0.8 and reduced ϵ linearly from 0.2 to 0.0 over the course of 30,000 episodes. In total, the agent was trained for 76,800 episodes. The target network update parameters were $C = 1$ and $\tau = 0.00005$.

G. Evaluation procedure

We evaluated the trained agents on 192 episodes which were generated with an independent set of talkers. We report success rate (percentage of episodes in which the agent successfully oriented towards the talker location), Chebyshev distance at

TABLE II
GENERALIZATION ACROSS ACOUSTIC ENVIRONMENTS

Training environment	Testing environment	Success rate %	Chebyshev distance	Episode length
Anechoic	Low reverb	62.5	0.8	13.6
	Med reverb	46.4	1.9	15.0
	High reverb	29.7	2.7	16.4
Low reverb	Anechoic	71.4	0.5	12.8
	Med reverb	35.9	1.8	16.0
	High reverb	25.0	3.0	17.1
Med reverb	Anechoic	56.2	0.9	14.3
	Low reverb	60.9	0.7	13.5
	High reverb	41.7	1.6	15.5
High reverb	Anechoic	32.8	1.3	16.8
	Low reverb	48.4	1.0	14.5
	Med reverb	58.3	0.7	14.0

the end of each episode (that is, the number of actions needed to reduce the orientation deviation to zero), and episode length (that is, the average number of actions). The performance of trained agents was compared to the performance of an agent behaving at random.

IV. EXPERIMENTS AND RESULTS

A. Audio-driven head-orientation within training environment

The evolution of the Chebyshev distance metric shows that the audio-driven DQN agents learned to orient towards a talker over the course of training, both in anechoic and in naturalistic environments with reverberation (Fig. 2). Evaluating the trained agents on the independent test episodes demonstrated that the RL agent trained on anechoic environments was highly successful at the task: the agent oriented towards the talker location on 100 % of the episodes (average remaining Chebyshev distance = 0.0), taking an average of 4.3 actions to reach the target (Table. I, average shortest sequences = 3.4).

Performance was notably lower when the audio-driven DQN agent was trained on naturalistic environments with reverberation: In the presence of low, medium or high reverberation, the agent's success rate dropped to 66.7 %, 57.3 %, and 57.8 %, respectively (Table. I). Nevertheless, for episodes in which the agent did not reach the target orientation, the final orientation deviation was small: the remaining Chebyshev distance was < 1 for all naturalistic acoustic environments (Table. I). Moreover, our audio-driven DQN approach still substantially outperformed an agent performing at random (success rate = 27.6 %).

B. Generalization across acoustic scenes

To evaluate to what degree the audio-driven DQN agents generalise across acoustic environments, we evaluated performance of the trained agents in environments with reverberation properties that deviated from the training environment (i.e., in out-of-distribution settings). Table. II and Fig. 4 show that the performance of the agent trained on anechoic environments was substantially lower in naturalistic environments with reverberation. Specifically, there was an inverse relationship

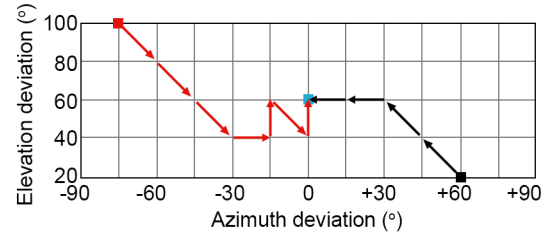


Fig. 3. Example of two trajectories of the trained DQN agents. Black arrows: trajectory of an agent trained on anechoic environments. Red arrows: trajectory of an agent trained on a high reverb environment.

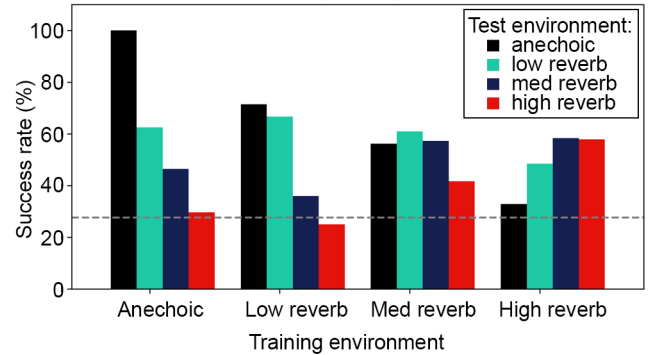


Fig. 4. generalization across acoustic environments. Bars reflect the performance of the trained agent on the evaluation episodes for each of the acoustic environments. Dashed line indicates success rate of random agent.

between reverberation strength in the testing environment and performance of the agent trained on anechoic environments.

Overall, the results indicate that agents generalise to acoustic environments with less reverberation than the environment they were trained on, but not to environments with more reverberation. For example, the DQN agent trained on medium reverb environments achieved a comparable success rate in anechoic and low-reverb environments, but performed at the level of the random agent in high reverb environments (Fig. 4). Finally, the agent trained on high reverb environments did not perform well in anechoic environments (Table. II, Fig. 4).

V. CONCLUSION

We introduced a novel audio-driven DRL approach for head-orientation control in the context of human-robot interaction. The autonomous agent achieved near perfect performance in anechoic environments. While the presence of reverberation in naturalistic acoustic environments affected the agent's performance, the agent substantially outperformed an agent behaving at random in such reverberant environments. Further, our results show that trained agents generalise to environments with less reverberation than the training environment. In summary, we show that audio-driven DRL is a promising approach to create autonomous systems that learn directly from sound signals in the environment.

REFERENCES

[1] Admoni, H., and Scassellati, B. (2017). Social eye gaze in human-robot interaction: a review. *Journal of Human-Robot Interaction*, 6(1), 25-63.

[2] Kompatsiari, K., Tikhonoff, V., Ciardo, F., Metta, G., and Wykowska, A. (2017). The importance of mutual gaze in human-robot interaction. In *Social Robotics: 9th International Conference, ICSR 2017, Tsukuba, Japan, November 22-24, 2017, Proceedings* 9 (pp. 443-452). Springer International Publishing.

[3] Arulkumaran, K., Deisenroth, M. P., Brundage, M., and Bharath, A. A. (2017). Deep reinforcement learning: A brief survey. *IEEE Signal Processing Magazine*, 34(6), 26-38.

[4] Lathuilière, S., Massé, B., Mesejo, P., and Horaud, R. (2019). Neural network based reinforcement learning for audio-visual gaze control in human-robot interaction. *Pattern Recognition Letters*, 118, 61-71.

[5] Zhu, K., and Zhang, T. (2021). Deep reinforcement learning based mobile robot navigation: A review. *Tsinghua Science and Technology*, 26(5), 674-691.

[6] Zhu, Y., Mottaghi, R., Kolve, E., Lim, J. J., Gupta, A., Fei-Fei, L., and Farhadi, A. (2017, May). Target-driven visual navigation in indoor scenes using deep reinforcement learning. In *2017 IEEE international conference on robotics and automation (ICRA)* (pp. 3357-3364). IEEE.

[7] Zeng, F., Wang, C., and Ge, S. S. (2020). A survey on visual navigation for artificial agents with deep reinforcement learning. *IEEE Access*, 8, 135426-135442.

[8] Chen, C., Jain, U., Schissler, C., Gari, S. V. A., Al-Halah, Z., Ithapu, V. K., ... and Grauman, K. (2020). Soundspaces: Audio-visual navigation in 3d environments. In *Computer Vision–ECCV 2020: 16th European Conference, Glasgow, UK, August 23–28, 2020, Proceedings, Part VI* 16 (pp. 17-36). Springer International Publishing.

[9] Younes, A., Honerkamp, D., Welschehold, T., and Valada, A. (2023). Catch me if you hear me: Audio-visual navigation in complex unmapped environments with moving sounds. *IEEE Robotics and Automation Letters*, 8(2), 928-935.

[10] Giannakopoulos, P., Pikrakis, A., and Cotronis, Y. (2021, June). A deep reinforcement learning approach to audio-based navigation in a multi-speaker environment. In *ICASSP 2021-2021 IEEE International Conference on Acoustics, Speech and Signal Processing (ICASSP)* (pp. 3475-3479). IEEE.

[11] Giannakopoulos, P., Pikrakis, A., and Cotronis, Y. (2021). A Deep Reinforcement Learning Approach for Audio-based Navigation and Audio Source Localization in Multi-speaker Environments. *arXiv preprint arXiv:2110.12778*.

[12] Latif, S., Cuayáhuitl, H., Pervez, F., Shamshad, F., Ali, H. S., and Cambria, E. (2023). A survey on deep reinforcement learning for audio-based applications. *Artificial Intelligence Review*, 56(3), 2193-2240.

[13] Mnih, V., Kavukcuoglu, K., Silver, D., Rusu, A. A., Veness, J., Bellemare, M. G., ... and Hassabis, D. (2015). Human-level control through deep reinforcement learning. *nature*, 518(7540), 529-533.

[14] van der Heijden, K., Rauschecker, J. P., de Gelder, B., and Formisano, E. (2019). Cortical mechanisms of spatial hearing. *Nature Reviews Neuroscience*, 20(10), 609-623.

[15] Han, C., Luo, Y., and Mesgarani, N. (2021). Binaural Speech Separation of Moving Speakers With Preserved Spatial Cues. In *Interspeech* (pp. 3505-3509).

[16] Cobbe, K., Klimov, O., Hesse, C., Kim, T., and Schulman, J. (2019, May). Quantifying generalization in reinforcement learning. In *International conference on machine learning* (pp. 1282-1289). PMLR.

[17] Panayotov, V., Chen, G., Povey, D., and Khudanpur, S. (2015, April). Librispeech: an asr corpus based on public domain audio books. In *2015 IEEE international conference on acoustics, speech and signal processing (ICASSP)* (pp. 5206-5210). IEEE.

[18] Majdak, P., Iwaya, Y., Carpentier, T., Nicol, R., Parmentier, M., Roginska, A., ... and Noisternig, M. (2013, May). Spatially oriented format for acoustics: A data exchange format representing head-related transfer functions. In *Audio Engineering Society Convention 134. Audio Engineering Society*.

[19] Scheibler, R., Bezzam, E., and Dokmanić, I. (2018, April). Pyroomacoustics: A python package for audio room simulation and array processing algorithms. In *2018 IEEE international conference on acoustics, speech and signal processing (ICASSP)* (pp. 351-355). IEEE.

[20] Amengual Gari, S. V., Arend, J. M., Calamia, P. T., and Robinson, P. W. (2021). Optimizations of the spatial decomposition method for binaural reproduction. *Journal of the Audio Engineering Society*, 68(12), 959-976.

[21] Sutton, R. S., and Barto, A. G. (2018). Reinforcement learning: An introduction. MIT press.

[22] Jaakkola, T., Singh, S., and Jordan, M. (1994). Reinforcement learning algorithm for partially observable Markov decision problems. *Advances in neural information processing systems*, 7.

[23] Huber, P. J. (1992). Robust estimation of a location parameter. In *Breakthroughs in statistics: Methodology and distribution* (pp. 492-518). New York, NY: Springer New York.

[24] Lillicrap, T. P. (2015). Continuous control with deep reinforcement learning. *arXiv preprint arXiv:1509.02971*.

[25] Paszke, A., Gross, S., Massa, F., Lerer, A., Bradbury, J., Chanan, G., ... and Chintala, S. (2019). Pytorch: An imperative style, high-performance deep learning library. *Advances in neural information processing systems*, 32.

[26] Loshchilov, I. (2017). Decoupled weight decay regularization. *arXiv preprint arXiv:1711.05101*.